

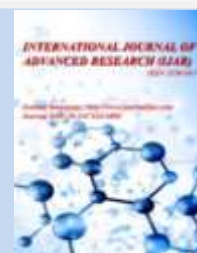


Journal Homepage: -[www.journalijar.com](http://www.journalijar.com)

## INTERNATIONAL JOURNAL OF ADVANCED RESEARCH (IJAR)

Article DOI:10.21474/IJAR01/15258

DOI URL: <http://dx.doi.org/10.21474/IJAR01/15258>



### RESEARCH ARTICLE

#### OXIDATIVE BALANCE IN BRAIN AFTER CHRONIC EXPOSURE TO ARSENIC

Julián G. Bonetto<sup>1,2</sup> and Susana Puntarulo<sup>1,2</sup>

1. Universidad de Buenos Aires. Facultad de Farmacia y Bioquímica, Fisicoquímica. Buenos Aires, Argentina.
2. Conicet-Universidad de Buenos Aires. Instituto de Bioquímica y Medicina Molecular (IBIMOL). Buenos Aires, Argentina.

#### Manuscript Info

##### Manuscript History

Received: 26 June 2022

Final Accepted: 28 July 2022

Published: August 2022

##### Key words:-

Antioxidants, Arsenic, Brain, Lipid Peroxidation, Oxidative Balance In The Hydrophilic Cellular Medium, Oxidative Balance In The Lipophilic Cellular Medium

#### Abstract

The effect of chronic As exposure in brain, the specific oxidants production and oxidative stress still needs more attention. In the present study, male wistar rats were chronically exposed to As by the drinking water during 60 days. The rats receiving a dose of 10 mg As/l showed a 9- and 18-fold increase in the content of As in blood and brain, respectively, as compared to the control group. Histopathological changes were detected in brain samples isolated from animals treated with As as compared to control animals. The oxidation rate of 2',7'-Dichlorofluorescein diacetate (DCFH-DA) showed no significant changes after the treatment. A significant increase (13%) in the steady state concentration of ascorbyl radical (A<sup>•</sup>) was determined in the brain isolated from animals exposed to 50 mg As/l. The lipid radical (LR<sup>•</sup>) generation rate and the content of malondialdehyde (MDA) were increased by 34% and 32%, respectively in brain isolated from rats receiving 50 mg As/l. The content of ascorbate (AH) in brain was not affected by the exposure to As. However, the content of glutathione (GSH) and the lipophilic antioxidant  $\alpha$ -tocopherol ( $\alpha$ -T), were significantly decreased after As supplementation, as compared to control brains. The A<sup>•</sup>/AH<sup>-</sup> content ratio in rat brain showed no changes associated to the As supplementation. Nevertheless, a significant increase of 44% and 55% was determined in the LR<sup>•</sup>/ $\alpha$ -T and MDA/ $\alpha$ -T content ratios, respectively, suggesting that the oxidative imbalance in the lipophilic cellular medium could be the primarily effect of As associated to membrane damage.

Copy Right, IJAR, 2022., All rights reserved.

#### Introduction:-

Arsenic (As) is a common metalloid in the crust of the earth with both metallic and non-metallic chemical characteristic. It is widely used in industries-like metal alloys, electronic circuitry, paints, pesticides, wood preservatives and, in medicine, for the treatment of a special type of acute myeloblastic leukemia, and for skin lesion in traditional Chinese medicine (Palma-Lara et al., 2020; Zheng et al., 2019). The effect of exposure to As was studied in a variety of experimental models and whole organism (i.e. human, animal, plant), and/or populations for several decades. Plenty information in relation to acute As poisoning reported that it could derive in vomit, bloody diarrhea, skin ulceration, hypovolemic shock and death in less than a week (Zheng et al., 2019). In the other hand, chronic As exposure through natural (i.e. drinking water) or anthropogenic (i.e. metal mining, burning of fossil

**Corresponding Author:- Susana Puntarulo**

Address:- Conicet-Universidad de Buenos Aires. Instituto de Bioquímica y Medicina Molecular (IBIMOL). Buenos Aires, Argentina.

fuels) sources has been associated with skin, bladder, and lung cancer; hepatic-, hematologic-, respiratory-, renal-, cardiovascular- and neurologic-diseases (i.e. Alzheimer, Parkinson, Dementia) (Bonetto et al., 2017; World Health Statistics, 2017; Dani and Walter, 2018). Up to now, the complex network of the mechanism(s) responsible for the response to As, and the participation of oxidative stress in these effects are still under discussion.

In the last decade, many research groups studying As-dependent biological impairment considered the oxidative and nitrosative stress as an important factors contributing to the final observed effect in the living organisms (Hu et al., 2020; Thakur et al., 2021). As exposure could generate different types of reactive oxygen species (ROS) and reactive nitrogen species (RNS) in a variety of experimental models of diseases (Jomova et al., 2011). Changes in the content of antioxidants like as glutathione (GSH), and antioxidant enzymes activities such as superoxide dismutase (SOD), catalase (CAT), GSH reductase (GR), glutathione-S-transferase (GST) and GSH peroxidase (GPx) were characterized in different As exposure experimental models (Flora, 2011; Bharti et al., 2012). Chandravanshi et al. (2018) reported abrupt changes in ROS production, oxidative stress and mitochondrial functions in different brain regions in neurotoxicity develop by As. Wang et al. (2015) suggested changes in the hippocampal morphology by disturbing normal apoptotic regulatory pathways in neural cells of hippocampus on subchronic As exposed rats. Increase in lipid peroxidation and lipophilic antioxidant content depletion was also observed in rat brain, heart and liver exposed to As (Flora et al., 2007; Bharti, 2012) in several experimental models including exposure of rats to 100 p.p.m. of As in drinking water for 28 days. Li et al. (2021) reported an increase in lipid peroxidation, inducible nitric oxide synthetase (iNOS) activity, and NO levels in brain after chronic exposure to As. Moreover, low levels of the activities of the antioxidant enzymes SOD, CAT, GR, GST and GPx activity were shown in the brain of subchronic As exposed animals (Li et al., 2021), decrease in acetylcholinesterase activity and histopathological changes in brain including neuronal degeneration and necrosis, gliosis, neuronophagia and spongiosis in a dose related manner in chronic exposure animals by the drinking water (Singh et al., 2020). However, it seems that an experimental model that resembles accurately the effect of As in humans is not currently available. Wang et al (2002) summarized successful studies in carcinogenesis using the most common strains of rats and mice. New evidence of the specific radical species generation in As acute exposure employing ex vivo and in vivo experimental models was presented by Bonetto et al. (2017). The oxidative stress balance in the hydrophilic cellular environment of the brain assessing the ascorbyl radical (A<sup>•</sup>)/ascorbate (AH) content ratio, and the lipid radical (LR<sup>•</sup>)/ $\alpha$ -tocopherol ( $\alpha$ -T) content ratio for evaluation of the oxidative stress index in the lipophilic cellular environment was described. An increase in the LR<sup>•</sup>/ $\alpha$ -T ratio, but not in the A<sup>•</sup>/AH ratio, was reported in brain of both ex vivo and in vivo acute exposure to As. Moreover, a different response in the content of highly relevant antioxidants such as GSH, was described depending on the via through which As reaches the brain, even when the tissue final steady state concentration of the toxic was similar (Bonetto et al., 2017).

The hypothesis of the present work is that chronic As administration is responsible for oxidative imbalance in the lipophilic cellular environment causing membrane deterioration and cellular injury in rat brain. The effect of in vivo chronic exposure to As by the drinking water was studied by histopathology, the oxidation rate of 2',7'-Dichlorofluorescein diacetate (DCFH-DA) (as a marker of generation of oxidant species), the rate of generation of LR<sup>•</sup> and A<sup>•</sup> by EPR methodology, MDA content by HPLC, and the content of non-enzymatic antioxidant capacity in the rat brain.

## Material and Methods:-

### Animal and experimental design

The male Albino Wistar rats (initial weight  $60 \pm 5$  g) used in this study were provided by the Animal Facility of the School of Pharmacy and Biochemistry, University of Buenos Aires. The animals were housed under standard conditions of light, temperature and humidity with ad libitum access to water and food. After weaning, the animals were randomized into three groups (n=6): Group I rats served as the control group and were feed standard rat chow and water; Group II received standard rat chow and sodium arsenite equivalent to 10 mg As/l (10 p.p.m.) in the drinking water, and Group III received standard rat chow and sodium arsenite equivalent to 50 mg As/l (50 p.p.m.) in the drinking water. After 60 days of treatment, the animals were euthanized in a CO<sub>2</sub> chamber. Brain or/and liver from control and As-treated animals were excised and rinsed in cold saline solution. Except where noted otherwise, the samples were frozen-clamped immediately and stored under liquid N<sub>2</sub> until used. Whole blood was taken by cardiac puncture. The procedures received approval from the Institutional Animal Care and Use Committee-School of Pharmacy and Biochemistry (CICUAL-FFyB, RES N°1037), according to the Guide for the Care and Use of Laboratory Animals (1985) and with the principles and directives of the European Communities Council Directives (1986).

**As content in tissue**

The quantification of As species [ $\text{As}^{\text{V}}$ + $\text{As}^{\text{III}}$ +monomethylarsonic acid (MMA)+dimethyl arsinic acid (DMA)] content in brain and whole blood was performed by hydride generation coupled to atomic absorption spectrometry (HG-AAS), after dry mineralization. A hydride generator VGA77 and an atomic absorption spectrometer Varian Spectra AA 200 was employed according to Navoni et al. (2010).

**Determination of 2',7'-Dichlorofluorescein diacetate (DCFH-DA) oxidation rate**

Brain tissue (250 mg FW per ml) was homogenized in 100 mM Tris-HCl buffer solution pH 7.2 with EDTA 2 mM and  $\text{MgCl}_2$  5 mM. The reaction mixture containing 8  $\mu\text{l}$  of brain homogenates (approximately 7 mg/ml), 3  $\mu\text{l}$  DCFH-DA solution (1 mg/ml) in pure methanol and 239  $\mu\text{l}$  of HEPES buffer per well, was incubated for the indicated periods at 37°C. Samples fluorescence was determined and quantified using a Varioskan LUX microplate reader at  $\lambda_{\text{ex}}=488$  nm and  $\lambda_{\text{em}}=525$  nm.

**Histopathology**

Brain or liver rat samples were obtained and fixed for light microscopy and for high resolution light microscopy (HRLM) according to Bonetto et al. (2020). A Digital Pathology Slide Scanner Scope Leica Biosystems Aperio CS2 (USA) was used for observation of the samples.

**Detection of  $\text{A}^{\bullet}$  content by EPR**

Brain tissue was homogenized in dimethyl sulfoxide (DMSO) to a final concentration of 25 mg/ml, and a Bruker EMX plus X band spectrometer was used for  $\text{A}^{\bullet}$  measurements. The spectra were immediately scanned under the following conditions: 50 kHz field modulation, room temperature, microwave power 10 mW, modulation amplitude 1 G, time constant 655 ms, receiver gain  $1 \times 10^5$ , microwave frequency 9.81 GHz, and scan rate 0.18 G/s (Piloni and Puntarulo, 2016). Quantification was performed as previously described, according to Kotake et al. (1996).

**Detection of  $\text{LR}^{\bullet}$  generation rate by EPR**

$\text{LR}^{\bullet}$  generation rate was detected by a spin trapping technique using N-t-butyl- $\alpha$ -phenyl nitron (PBN). Brain tissue was homogenized in 40 mM PBN prepared in DMSO immediately prior to use in a concentration of 25 mg of tissue per ml, incubated for 30 min, and immediately transferred to a Pasteur pipette for  $\text{LR}^{\bullet}$  detection. Instrument settings were as follows: modulation frequency 50 kHz, microwave power 10 mW, microwave frequency 9.75 GHz, centered field 3487 G, time constant 81.92 ms, modulation amplitude 1.20 G and sweep width 100 G, according to Lai et al. (1994). Quantification of the spin adduct was performed using TEMPO introduced into the same sample cell used for spin trapping. EPR spectra for both sample and TEMPO solutions were recorded at the same spectrometer settings and the first derivative EPR spectra were double integrated to obtain the area intensity, then the concentration of spin adduct was calculated according to Kotake et al. (1996).

**MDA content**

MDA content in brain was performed using HPLC according to Candan and Tuzmen (2008). The equipment was a Hewlett-Packard serie 1100 HPLC with fluorescent detector with the following chromatography parameters: Supelco SUPELCOSIL LC-18-DB 15 cmx4.6 mmx5  $\mu\text{m}$  column; mobile phase: buffer  $\text{KH}_2\text{PO}_4$  50 mM pH 6.8: methanol (60:40); detector setting:  $\lambda_{\text{ex}}=532$  nm and  $\lambda_{\text{em}}=553$  nm. Sigma 1,1,3,3-tetraethoxypropane was used as standard.

**Reduced GSH content**

The content of GSH in brain exposed to As was performed according to Rodriguez-Ariza et al. (1994) with modifications. Brain homogenates (20% w/v) were prepared in 1 M perchloric acid and 2 mM EDTA, immediately after isolation of the rat brain. After precipitation at 10,000g for 5 min at 4°C, the supernatant was recovered and filtered using 0.2  $\mu\text{m}$  filters. The samples were kept at -80°C for quantification by HPLC-EQ assay employing commercially available standard GSH.

**AH<sup>-</sup> content**

Brain samples were homogenized in metaphosphoric acid (10%, w/v) and the content of  $\text{AH}^-$  was measured by reverse-phase HPLC-EQ according to Kutnink et al. (1987).

**$\alpha$ -T content**

The content of  $\alpha$ -T in brain tissues was quantified by reverse-phase HPLC-EQ with a Perkin Elmer 250 pump and a ESA Cuolochem II electrochemical detector, at an applied oxidation potential of 0.6 V according to Desai (1984).  $\alpha$ -T (Sigma) was used as standard.

**Statistical analyses**

Data in the text and tables are expressed as mean values  $\pm$  standard error of the mean (S.E.M.). Statistical tests were carried out using Graph Pad Prism 6, employing Kruskal Wallis for statistical difference, with a level of statistical significance of  $p < 0.01$ .

**Results:-**

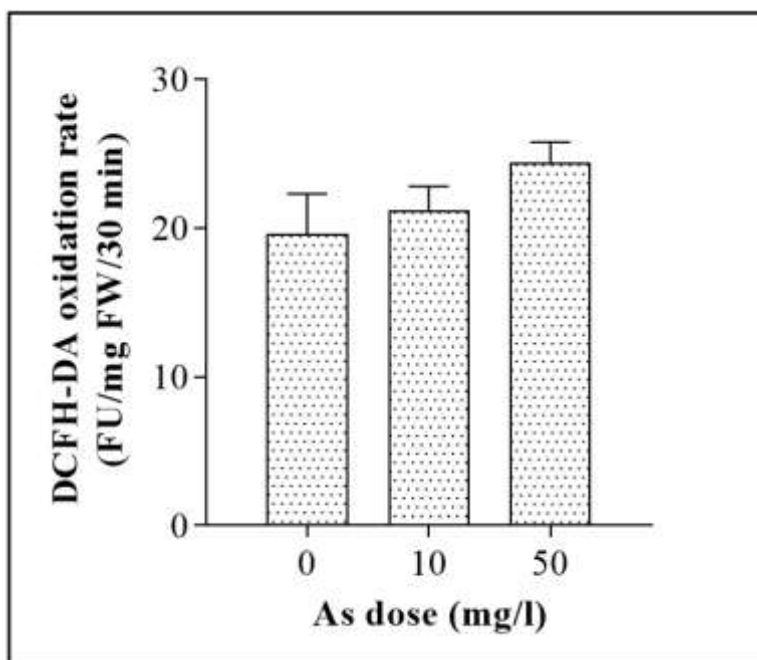
Chronic exposure of the animals to As in the drinking water during 60 days did not significantly modified neither the weight of the body nor the weight of the brain of the animals, as compared to the control group (data not shown). The rats receiving a dose of 10 mg As/l showed a 9- and 18-fold increase in the content of As in blood and brain, respectively, as compared to the control group. The animal group receiving 50 mg As/l in the drinking water for 60 day increased by 13- and 36-fold in the content of As in blood and brain, respectively, as compared to the control group (Table 1), showing a dose-dependent accumulation of As in the studied tissues.

**Table 1:-** As content in blood and brain of rats exposed for 60 days to chronic exposure.

| Dose       | As concentration in blood (nmol As/ml) | As concentration in brain (pmol As/mg FW) | Total As content in blood ( $\mu$ g) | Total As content in brain ( $\mu$ g) |
|------------|--|---|--------------------------------------|--------------------------------------|
| Control    | $0.13 \pm 0.03$                        | n.d.                                      | $0.26 \pm 0.07$                      | n.d.                                 |
| 10 mg As/l | $9 \pm 1^*$                            | $18 \pm 5^*$                              | $16 \pm 1^*$                         | $2.5 \pm 0.7^*$                      |
| 50 ml As/l | $13 \pm 2^*$                           | $35 \pm 6^*$                              | $23 \pm 3^*$                         | $4.9 \pm 0.9^*$                      |

\*significant different as compared with control,  $p < 0.01$ .

The DCFH-DA oxidation rate was employed as a marker of generation of oxidant species in the rat brain after receiving As during 60 days. No significant changes in the DCFH-DA oxidation rate in the brain isolated from animals exposed to either 10 or 50 mg As/l, as compared to the control group were observed (Fig. 1).

**Figure 1:-** DCFH-DA oxidation rate in brain after 60 days of chronic exposure to As by the drinking water.

The morphological characteristics of both, brain and liver, were studied by observation of the histopathological features of tissues slices stained with haematoxylin-eosin using HRLM in either control or tissue isolated from animals treated with As (Fig. 2). The observation of the liver of the animals chronically exposed to 50 mg As/l in the drinking water showed focal necrosis of the tissue (circle 1), vacuolar and microvacuolar degeneration (black arrows) and a remarkable disarray of the trabecular structure (circle 2) (Fig. 2B). In agreement with previous observations in animals exposed chronically to As, these observations suggested damage in the liver by the treatment, as compared to liver from control animals (Fig. 2A). The morphology of the brain samples isolated from control animals (Fig. 2C) was significantly modified in samples isolated from animals treated with As. Data shown in the figure 2D, indicated the presence of neuronal cells (circle 3) with nuclear condensation, cytoplasmic retraction and pericellular edema.

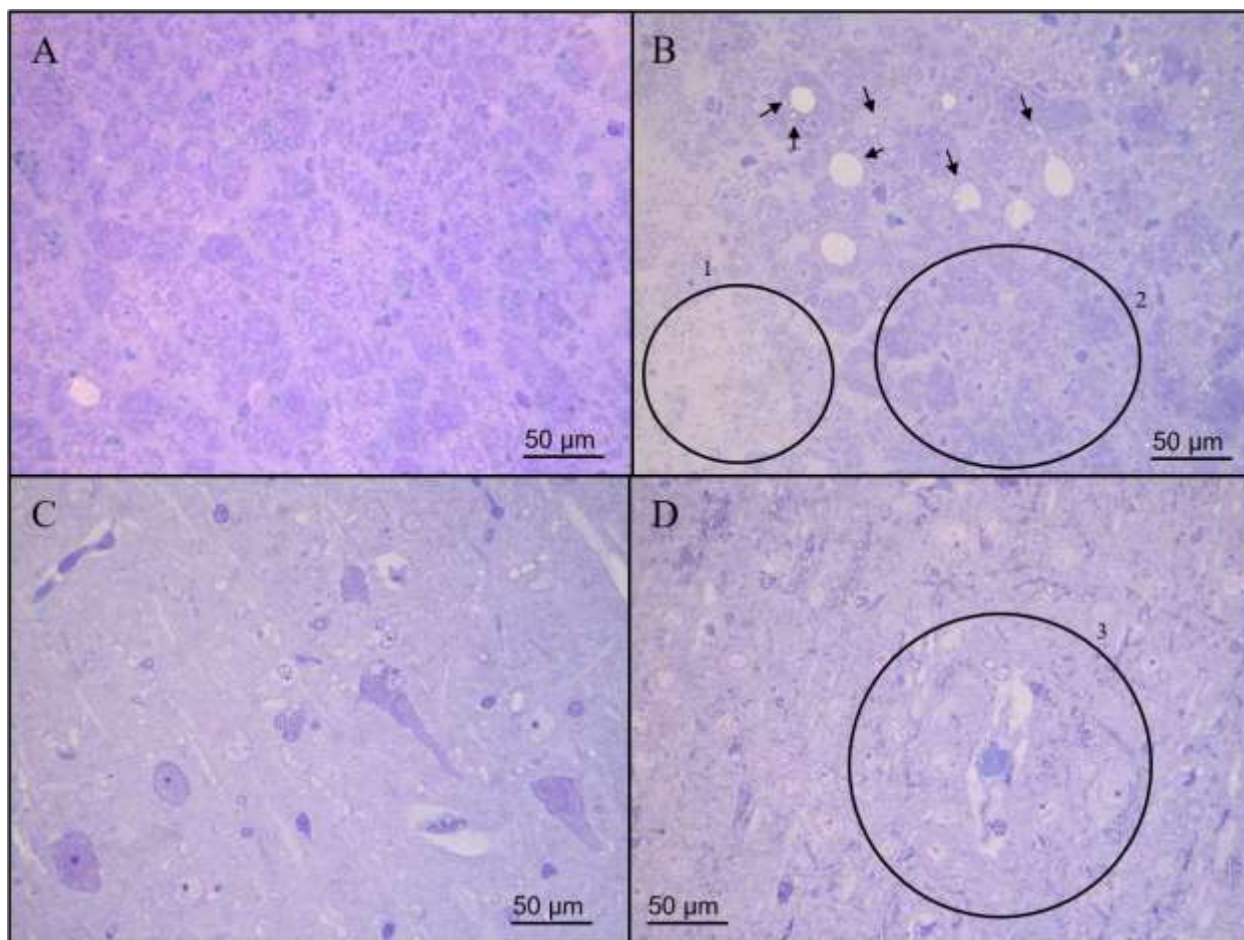


**Figure 2:-** Histopathology. HRLM in liver and brain slices stained with haematoxylin-eosin. **A.** Control rat liver; **B.** Rat liver after 60 days of exposure to 50 mg As/l in the drinking water: focal necrosis (circle 1), vacuolar and microvacuolar degeneration (black arrows) and disarray on the trabecular structure (circle 2); **C.** Control rat brain; **D.** Rat brain after 60 days of exposure to 50 mg As/l in the drinking water: neuronal cells with nuclear condensation, cytoplasmic retraction and pericellular edema(circle 3).

A typical EPR spectrum for  $A^{\bullet}$  was measured in brain samples isolated from both, control and As treated-rats (Fig. 3A). By the quantification of the obtained EPR spectra, a significant increase (13%) in the steady state concentration of  $A^{\bullet}$  was determined in the brain isolated from animals exposed to 50 mg As/l (Fig. 3B).

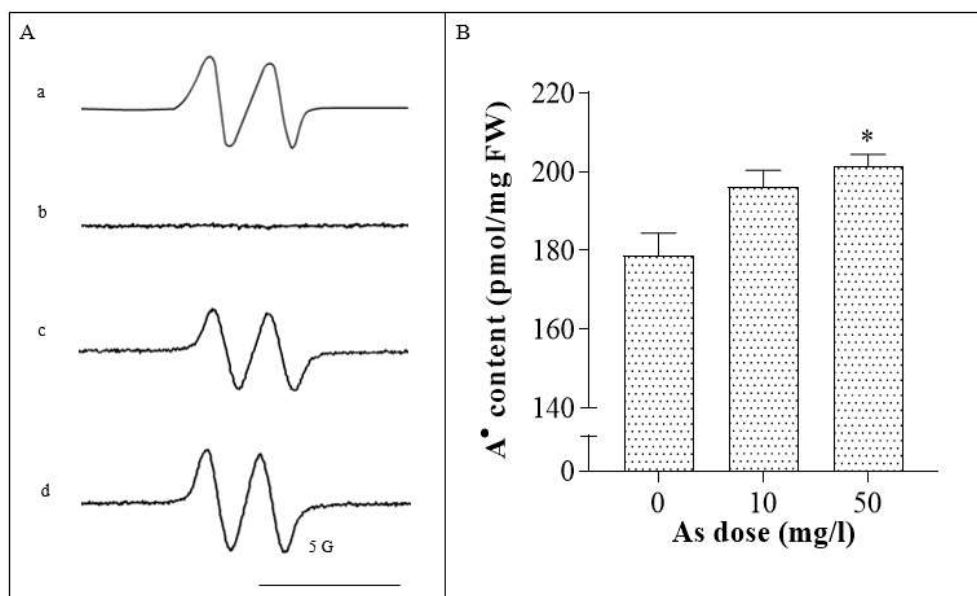


**Figure 3:-** A<sup>•</sup> radical content in brain after 60 days of chronic exposure to As. **A.** EPR spectrum for A<sup>•</sup> in brain: a) computer simulated-spectrum, b) DMSO alone, c) spectrum of A<sup>•</sup> in brain of control rat, d) spectrum of A<sup>•</sup> in brain of rat exposed to 50 p.p.m. of As. **B.** Quantification of A<sup>•</sup> radical content in brain after 60 days of chronic exposure to As.\*significant different as compared with control, p<0.01.

The LR<sup>•</sup> generation rate and the content of MDA were assessed as markers of lipid peroxidation in the brain. The typical EPR spectrum for LR<sup>•</sup> is shown in the figure 4A, and no significant modifications were determined in brain of treated animals with 10 As/l for 60 days. However, a significant increase of 34% was observed in the brain of rats receiving 50 mg As/l during the experimental treatment (Fig. 4B). The content of MDA, a final product of lipidperoxidation, showed the same profile with a significant increased of 32% in brain isolated from rats exposed to 50 mg As/l for 60 days (Fig. 4B).

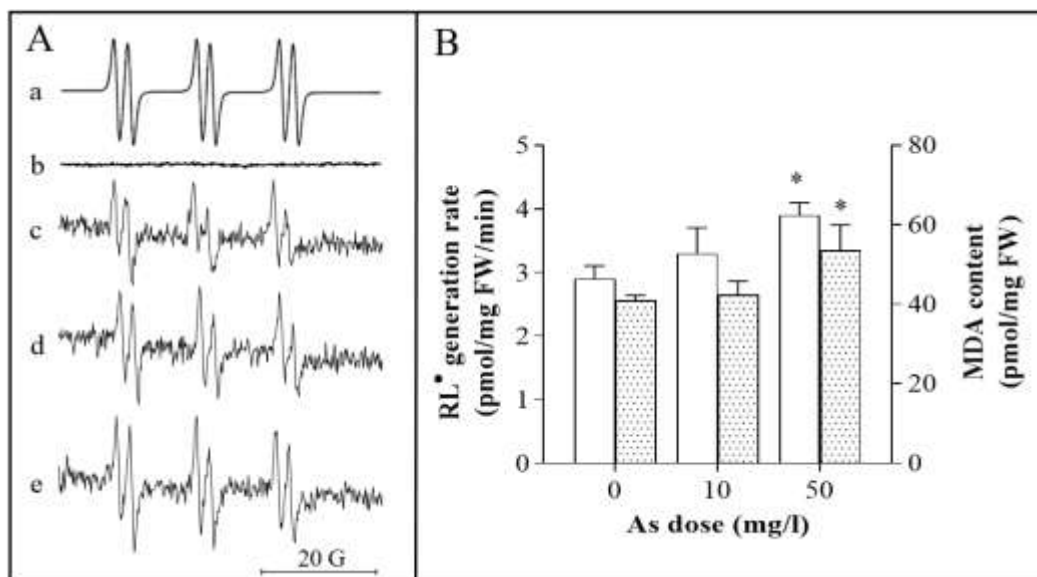


**Figure 4:-** LR<sup>•</sup> radical and MDA content in brain after 60 days of chronic exposure to As in the drinking water. **A.** EPR spectrum for LR<sup>•</sup> in brain: a) computer simulated-spectrum, b) PBN alone, c) spectrum of LR<sup>•</sup> in brain of control rat, d) spectrum of LR<sup>•</sup> in brain of rat exposed to 10 p.p.m. of As and e) spectrum of LR<sup>•</sup> in brain of rat exposed to 50 p.p.m. of As. **B.** Quantification of LR<sup>•</sup> generation rate (white bars) and MDA content (black bars) in brain after 60 days of chronic exposure to As.\*significant different as compared with control, p<0.01.

The content of the non-enzymatic antioxidants GSH,  $AH^+$  and  $\alpha$ -T, was determined in brain samples by HPLC methods, as previously stated. The content of  $AH^+$  in the brain of the rats exposed to As in neither of the tested doses was significantly altered as compared to brains from the control animals (Fig. 5A). The content of GSH was decreased by 15 and 25% after the supplementation of either 10 or 50 mg As/l in the drinking water during 60 days, respectively. A significant decrease of 9 and 17% in the content of the lipophilic antioxidant  $\alpha$ -T, was observed after the administration to the rats of either 10 and 50 mg As/l in the drinking water, respectively (Fig. 5B).

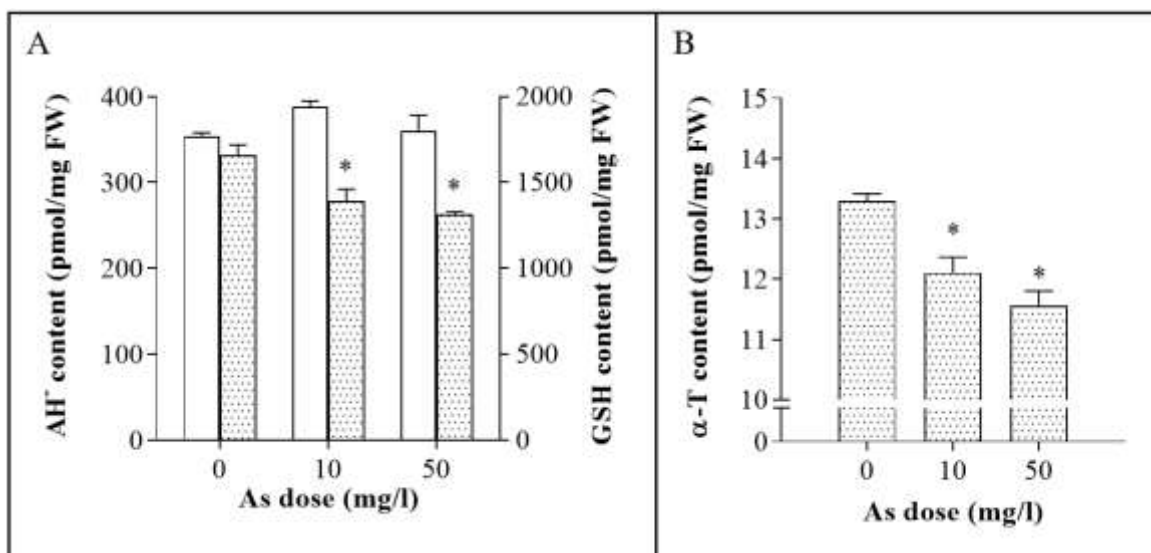


**Figure 5:-** Antioxidant content in rat brain after chronic exposure to As. **A.**  $AH^+$  content (white bars) and GSH (dot bars). **B.**  $\alpha$ -T content.\*significant different as compared with controls,  $p < 0.01$ .

The  $A^*/AH^+$  content ratio in rat brain, understood as an index of the oxidative balance in the hydrophilic cellular medium, showed no changes associated to the As supplementation to rats in the drinking water (Fig. 6A). However, a significant increase of 44 and 55% was determined in both, the  $LR^*/\alpha$ -T and  $MDA/\alpha$ -T content ratios, respectively (Fig. 6B), suggesting an alteration in the oxidative balance in the lipophilic cellular medium.

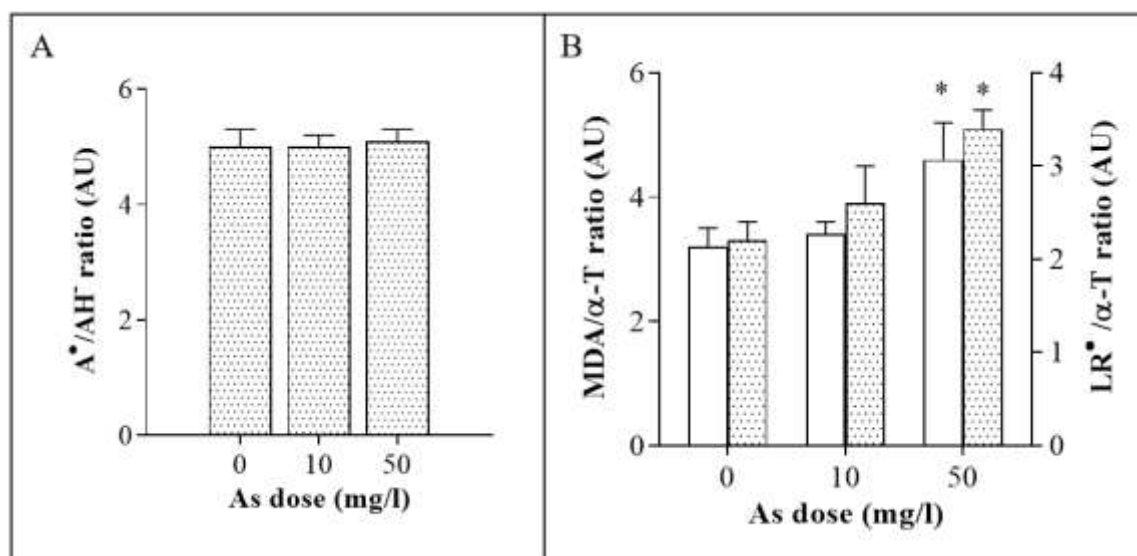


**Figure 6:-** Oxidative stress balance in brain after 60 days of chronic As exposure. **A.** Oxidative balance in hydrophilic cellular environment. **B.** Oxidative balance in lipophilic cellular environment assessed as  $MDA/\alpha$ -T content ratio (white bars) or  $LR^*/\alpha$ -T content ratio (dot bars).\*significant different as compared with controls,  $p < 0.01$ .

**Discussion:-**

Previous data from Bonetto et al. (2017) showed the specific radical generation in brain after ex vivo and acute in vivo exposure to As, where both,  $LR^*$  and  $LR^*/\alpha$ -T ratio, were increased in these experimental models. Although, in that study the amount of  $A^*$  radicals,  $AH^*$  and  $\alpha$ -T was not modified in brain after exposure to As, a significant decrease of GSH was measured only in the ex vivo model. The data reported here after chronic exposure to As showed that some oxidative parameters in rat brain were affected, as previously shown in the acute model. However, other alterations seem as specific features related to the experimental model of exposure. The administration of As by the drinking water, currently used as a good model for the uptake of As in biological organisms, initially damage the liver as shown in previous reports by Bi et al. (2022), among others, after generating its metabolites. The non-metabolized As, probably due by liver failure, might go to the brain leading to damage to the blood-brain barrier (BBB) that is a crucial immunological feature of the human central nervous system (CNS). Composed of many cell types, the BBB is both, a structural and a functional roadblock to microorganisms, such as bacteria, fungi, viruses or parasites, that may be circulating in the bloodstream (Dando et al., 2014; Chacko et al., 2022). As appears to be more actively accumulated in the brain of chronic As-exposed rats, as compared to the content of As found in brain after acute As exposure where approximately 0.1% of the amount of As in blood pass through the BBB (Bonetto et al., 2017). Manthari et al. (2018) associated the modifications on the BBB with an increase in the permeability of the brain to As. However, the  $A^*/AH^*$  ratio and the DCFH oxidation rate shown in the brain tissues were not modified by the experimental model of exposure to As, suggesting that the hydrophilic cellular environment of the brain could be more resilient to the deleterious effect of As toxicity.

The  $LR^*$  generation rate of the brain was increased after exposure to As in the three experimental models, suggesting that this is a common feature due to the presence of As, and an independent effect of the way that As reaches the brain. Regarding the antioxidant network activity, in the present study experimental evidence is presented showing that, even though  $AH^*$  content was not affected, both the content of GSH and  $\alpha$ -T was decreased in the brain of the animals receiving chronically As in the drinking water. It was previously reported that GSH that is one of cellular components with the major antioxidant capacity present in the organs of almost all animal species, plays a crucial role in the As metabolism (Bonetto et al., 2014). Using the acute model of administration of As, it was shown that the As could consume the GSH of the brain in an ex vivo exposure, even though the normal GSH brain content, at least, in the first 24 h after in vivo acute exposure to As was not compromised (Bonetto et al., 2017). The decrease in GSH content observed in this study might be caused by the As that is primarily metabolized in liver and reach the brain, either as As or As metabolites, in a first stage of the As exposure. In a more advanced stage of exposure, when the liver is severely damaged and the hepatic activity is compromised, the amount of non-metabolized As reaching the brain is even more significant and the consumption of the GSH present in this organ is significant. Furthermore, the content of  $\alpha$ -T that is required as a reduction agent for restoration, to maintain the membranes and the cellular viability in the brain affected by the oxidative imbalance in the lipophilic cellular environment of the brain, was shown to be decreased. As a consequence, the  $LR^*/\alpha$ -T ratio, understood as an indication of oxidative balance in the hydrophobic cellular medium, was compromised in all the experimental models (e.g. acute ex vivo, acute in vivo and chronic in vivo) of exposure to As, strongly suggesting that the primary effect of As might be associated to membrane damage.

Moreover, the deterioration of the BBB, a key factor to the normal function of the brain, caused by the presence of As and its metabolites plus the systemic interleukins produced by the damage, generate inflammation and might lead to oxidative damage in the brain cells. This effect on the permeability of the BBB could increase not only the amount of As in the brain, but also the uptake of systemic inflammatory mediators through the brain, intensifying the neuroinflammation and the neurovascular impact (Heusinkveld et al., 2016). Amal et al. (2020) showed that As in the drinking water or food, may affect the brain adversely and their proteomics and biochemical experiments in mice demonstrated that environmental levels of As induced dose-dependent biochemical changes. This statement is valid both, for toxic changes and the effects on the neuronal signaling. Mechanistically, As induced the release of  $Ca^{2+}$  that activated formation of nitric oxide (NO) by neuronal nitric oxide synthase (nNOS) activity, and promoted nitrosative modifications of proteins. Removal of As exposure reversed S-nitrosylation of the proteome to a "normal" SNO-proteome, suggesting that some neuropathologies that act through overproduction of NO might be ameliorated by reduction of those exposures. In brief, these observations that include the modification of  $Ca^{2+}$  levels, increases in NO, S-nitrosoglutathione (GSNO) and nitrated tyrosine ( $NO_2$ -Tyr) in brain, suggested an ineffective blocking of the uptake of As by the BBB, leading to developmental cognitive pathologies. Moreover, Bonetto et al. (2020) showed a significant increase in the  $LR^*$ , NO and  $NO_2$ -Tyr content in brain after acute in vivo exposure to As, with a remarkable decrease in the hippocampal pyramidal layer and in the number of pyramidal neurons in a

HLRM analysis of brain slices. In the *in vivo* chronic model shown here, after 60 days of chronic exposure to As by the drinking water, the deleterious effect on the liver and brain of the exposed animals was clearly observed in the histopathology analysed in the study by HLRM, probably by increase in NO production and pro-inflammatory mediators. More studies are necessary to elucidate this effects. The ability of NO to complex to Fe was previously described (Burov et al., 2022), and these complexes Fe-NO could be responsible to participate in the accumulation of NO inside of the cells (Burov et al., 2022). Fe, as part of the labile Fe pool (LIP) is highly reactive and can produce excessive ROS by Fenton reactions (Nishizaki and Iwahashi, 2015), resulting in cellular oxidative damage. However, the ability to catalyze lipid peroxidation of the Fe-NO complexes, understood as components of the LIP, is still not clear.

The lipid peroxidation of the membranes seems as a critical factor that might be reflected in the oxidative metabolism of Fe in the brain cells. Ferroptosis is a novel form of cell death triggered by lipid peroxidation in an Fe-dependent way (Dixon et al., 2012; Angeli et al., 2017; Gao and Jiang, 2018). In brief, ferroptosis is defined by three indispensable hallmarks, including the impaired lipid peroxide repair capacity caused by the loss of glutathione peroxidase 4 (GPX4) activity, the availability of redox-active Fe, and oxidation of polyunsaturated fatty acid (PUFA) containing phospholipids (Dixon and Stockwell, 2019). Currently, three biomarkers are available for identifying the occurrence of ferroptosis: protein marker (GPX4 and COX-2), lipid peroxidation, and lipid ROS (Li et al., 2017; Wang et al., 2017). Ferroptosis is supposed to be involved in the evolution of many diseases, including ischemia-reperfusion injury (Li et al., 2019), intracerebral hemorrhage (Li et al., 2017), and Parkinson's disease (Guiney et al., 2017). Bruni et al. (2018) indicated that ferritin-1 (Fer-1) or deferoxamine could improve human islet viability and function impaired by small molecules, in pancreatic disease. The evolution of ferroptosis lies at the intersection of amino acid, lipid, and Fe metabolism (Stockwell et al., 2017). Hence, the fine-tuning of Fe level is closely related to cellular ferroptosis. Wei et al., (2020) showed that the ferroptosis is involved in NaAsO<sub>2</sub>-induced pancreatic islet  $\beta$  cells dysfunction, and mitochondrial injury and degradation of Fe are responsible for the underlying molecular mechanism of ferroptosis. The diagram in figure 7 shows the hypothesis of the complex network triggered by As chronic administration and its effects on ROS generation, ferroptosis and inflammation. Further studies are required to respond the missing points and to help the understanding of the chronic As toxicity associated to oxidative stress that contributes to impairment of the brain function. This report is giving an oxidative scenario of the brain situation after chronic exposure to As by drinking water, and seems as a main issue to understand As effect on the oxidative balance that could be an interesting point to design strategies to control the possible toxicity of As in the water, in important areas where As is contributing to environmental pollution.

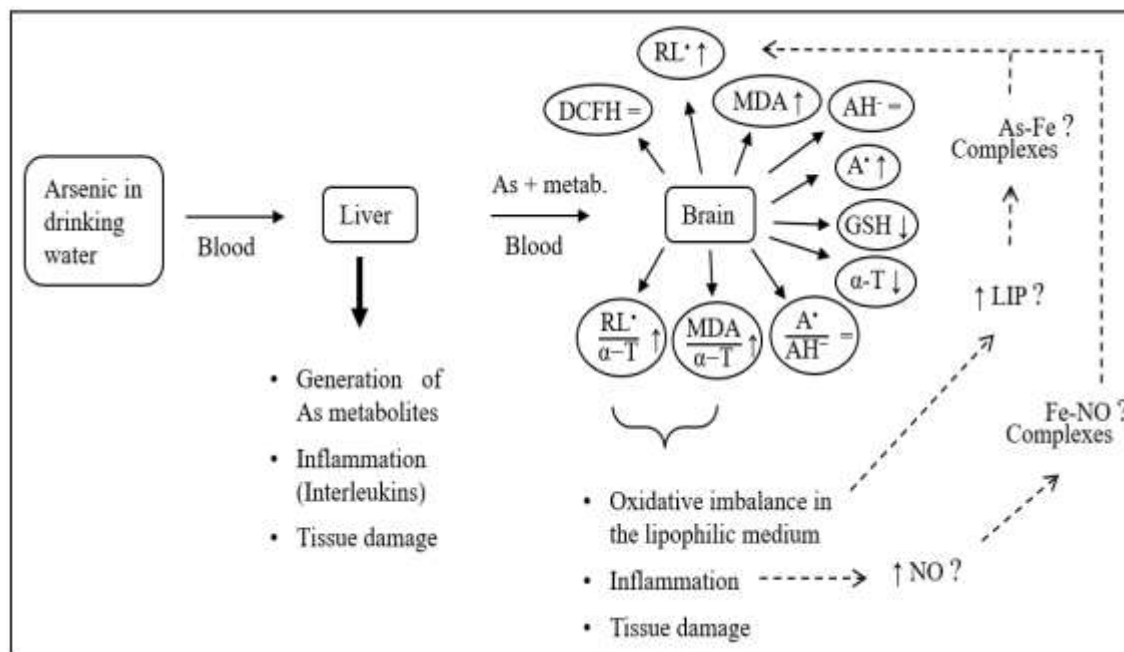


**Figure 7:-** Brief diagramme showing the As-dependent oxidative alterations in brain after chronic As administration. The circles indicate the parameters measured in this report and the point lines the proposed interections that could be triggered at the cellular brain level.

### Acknowledgements And Fundings:-

This study was supported by grants from the University of Buenos Aires (20020130100383BA), the National Council for Science and Technology (CONICET, PIP N°11220170100539CO) and National Agency for Scientific and Technological Promotion (ANPCyT, PICT-2020-SERIEA-03542).

### References:-

1. Amal, H., Gong, G., Yang, H., Joughin, B. A., Wang, X., Knutson, C. G., Kartawy, M., Khaliulin, I., Wishnok, J. S., & Tannenbaum, S. R. (2020). Low doses of arsenic in a mouse model of human exposure and in neuronal culture lead to S-Nitrosylation of synaptic proteins and apoptosis via nitric oxide. *Inter. J. Mol. Sci.*, 21(11), 3948. <https://doi.org/10.3390/ijms21113948>
2. Angeli, J. P. F., Shah, R., Pratt, D. A., & Conrad, M. (2017). Ferroptosis inhibition: Mechanisms and opportunities. *Trends Pharmacol. Sci.*, 38(5), 489–498. <https://doi.org/10.1016/j.tips.2017.02.005>
3. Bharti, V. K., Srivastava, R. S., Sharma, B., & Malik, J. K. (2012). Buffalo (*Bubalus bubalis*) epiphyseal proteins counteract arsenic-induced oxidative stress in brain, heart, and liver of female rats. *Biol. Trace Elem. Res.*, 146(2), 224–229. <https://doi.org/10.1007/s12011-011-9245-0>
4. Bi, D., Shi, M., Hu, Q., Wang, H., Lou, D., Zhang, A., & Hu, Y. (2022). LC/MS/MS-based liver metabolomics to identify chronic liver injury biomarkers following exposure to arsenic in rats. *Biol. Trace Elem. Res.* <https://doi.org/10.1007/s12011-021-03026-0>
5. Bonetto, J. G., Villaamil Lepori, E., & Puntarulo, S. (2014). Update on the oxidative stress associated with arsenic exposure. *Curr.Top. Toxicol.*, 10, 37–48.
6. Bonetto, J. G., Villaamil Lepori, E., & Puntarulo, S. (2017). Oxidative balance in brain after exposure to arsenic in ex vivo and in vivo models. *Int. J. Adv. Res.*, 5(10), 45–51. <https://doi.org/10.21474/IJAR01/5505>
7. Bonetto, J. G., Perazzo, J. C., & Puntarulo, S. (2020). Reactive nitrogen species in brain after in vivo exposure to arsenic. *Inter. J. Adv. Res.*, 8(6), 980–992. <https://doi.org/10.21474/IJAR01/11179>
8. Bruni, A., Pepper, A. R., Pawlick, R. L., Gala-Lopez, B., Gamble, A. F., Kin, T., Seeberger, K., Korbutt, G. S., Bornstein, S. R., Linkermann, A., & Shapiro, A. M. J. (2018). Ferroptosis-inducing agents compromise in vitro human islet viability and function. *Cell Death Dis.*, 9(6), 595. <https://doi.org/10.1038/s41419-018-0506-0>
9. Burov, O. N., Kletskii, M. E., Kurbatov, S. V., Lisovin, A. V., & Fedik, N. S. (2022). Mechanisms of nitric oxide generation in living systems. *Nitric Oxide*, 118, 1–16. <https://doi.org/10.1016/j.niox.2021.10.003>
10. Candan, N., & Tuzmen, N. (2008). Very rapid quantification of malondialdehyde (MDA) in rat brain exposed to lead, aluminium and phenolic antioxidants by high-performance liquid chromatography-fluorescence detection. *NeuroToxicology*, 29(4), 708–713. <https://doi.org/10.1016/j.neuro.2008.04.012>
11. Chacko, A., Delbaz, A., Choudhury, I. N., Eindorf, T., Shah, M., Godfrey, C., Sullivan, M. J., St John, J. A., Ulett, G. C., & Ekberg, J. A. K. (2022). *Streptococcus agalactiae* infects glial cells and invades the central nervous system via the olfactory and trigeminal nerves. *Front. Cell. Infec. Microbiol.*, 12, 793416. <https://doi.org/10.3389/fcimb.2022.793416>
12. Chandravanshi, L. P., Gupta, R., & Shukla, R. K. (2018). Developmental neurotoxicity of arsenic: Involvement of oxidative stress and mitochondrial functions. *Biol. Trace Elem. Res.*, 186(1), 185–198. <https://doi.org/10.1007/s12011-018-1286-1>
13. Dando, S. J., Mackay-Sim, A., Norton, R., Currie, B. J., St John, J. A., Ekberg, J. A. K., Batzloff, M., Ulett, G. C., & Beacham, I. R. (2014). Pathogens penetrating the central nervous system: infection pathways and the cellular and molecular mechanisms of invasion. *Clin. Microbiol. Rev.*, 27(4), 691–726. <https://doi.org/10.1128/CMR.00118-13>
14. Dani, S. U., & Walter, G. F. (2018). Chronic arsenic intoxication diagnostic score (CAsIDS). *J. Appl. Toxicol.*, 38(1), 122–144. <https://doi.org/10.1002/jat.3512>
15. Desai, I. D. (1984). [16] Vitamin E analysis methods for animal tissues. In *Methods in Enzymology* (pp. 138–147). [https://doi.org/10.1016/S0076-6879\(84\)05019-9](https://doi.org/10.1016/S0076-6879(84)05019-9)
16. Dixon, S. J., Lemberg, K. M., Lamprecht, M. R., Skouta, R., Zaitsev, E. M., Gleason, C. E., Patel, D. N., Bauer, A. J., Cantley, A. M., Yang, W. S., Morrison, B., & Stockwell, B. R. (2012). Ferroptosis: An Iron-dependent form of nonapoptotic cell death. *Cell*, 149(5), 1060–1072. <https://doi.org/10.1016/j.cell.2012.03.042>
17. Dixon, S. J., & Stockwell, B. R. (2019). The hallmarks of ferroptosis. *Ann.Rev. Cancer Biol.*, 3(1), 35–54. <https://doi.org/10.1146/annurev-cancerbio-030518-055844>
18. Flora, S. J. S., Bhadauria, S., Kannan, G. M., & Singh, N. (2007). Arsenic induced oxidative stress and the role of antioxidant supplementation during chelation: a review. *J. Envir. Biol.*, 28(2), 333–347. <http://www.ncbi.nlm.nih.gov/pubmed/17929749>

19. Flora, S. J. S. (2011). Arsenic-induced oxidative stress and its reversibility. *Free Radic. Biol. Med.*, 51(2), 257–281. <https://doi.org/10.1016/j.freeradbiomed.2011.04.008>
20. Gao, M., & Jiang, X. (2018). To eat or not to eat - the metabolic flavor of ferroptosis. *Curr. Opin. Cell Biol.*, 51, 58–64. <https://doi.org/10.1016/j.ceb.2017.11.001>
21. Guiney, S. J., Adlard, P. A., Bush, A. I., Finkelstein, D. I., & Ayton, S. (2017). Ferroptosis and cell death mechanisms in Parkinson's disease. *Neurochem. Int.*, 104, 34–48. <https://doi.org/10.1016/j.neuint.2017.01.004>
22. Heusinkveld, H. J., Wahle, T., Campbell, A., Westerink, R. H. S., Tran, L., Johnston, H., Stone, V., Cassee, F. R., & Schins, R. P. F. (2016). Neurodegenerative and neurological disorders by small inhaled particles. *NeuroToxicology*, 56, 94–106. <https://doi.org/10.1016/j.neuro.2016.07.007>
23. Hu, Y., Li, J., Lou, B., Wu, R., Wang, G., Lu, C., Wang, H., Pi, J., & Xu, Y. (2020). The role of reactive oxygen species in arsenic toxicity. *Biomolecules*, 10(2), 240. <https://doi.org/10.3390/biom10020240>
24. Jomova, K., Jenisova, Z., Feszterova, M., Baros, S., Liska, J., Hudecova, D., Rhodes, C. J., & Valko, M. (2011). Arsenic: toxicity, oxidative stress and human disease. *J. Appl. Toxicol.*, 31(2), 95–107. <https://doi.org/10.1002/jat.1649>
25. Kotake, Y., Tanigawa, T., Tanigawa, M., Ueno, I., Allen, D. R., & Lai, C.-S. (1996). Continuous monitoring of cellular nitric oxide generation by spin trapping with an iron-dithiocarbamate complex. *Biochim. Biophys. Acta Gen. Subj.*, 1289(3), 362–368. [https://doi.org/10.1016/0304-4165\(95\)00172-7](https://doi.org/10.1016/0304-4165(95)00172-7)
26. Kutnink, M. A., Hawkes, W. C., Schaus, E. E., & Omaye, S. T. (1987). An internal standard method for the unattended high-performance liquid chromatographic analysis of ascorbic acid in blood components. *Anal. Biochem.*, 166(2), 424–430. [https://doi.org/10.1016/0003-2697\(87\)90594-X](https://doi.org/10.1016/0003-2697(87)90594-X)
27. Lai, C.-S., & Komarov, A. M. (1994). Spin trapping of nitric oxide produced in vivo in septic-shock mice. *FEBS Lett.*, 345(2–3), 120–124. [https://doi.org/10.1016/0014-5793\(94\)00422-6](https://doi.org/10.1016/0014-5793(94)00422-6)
28. Li, Q., Han, X., Lan, X., Gao, Y., Wan, J., Durham, F., Cheng, T., Yang, J., Wang, Z., Jiang, C., Ying, M., Koehler, R. C., Stockwell, B. R., & Wang, J. (2017). Inhibition of neuronal ferroptosis protects hemorrhagic brain. *JCI Insight*, 2(7), e90777–e90777. <https://doi.org/10.1172/jci.insight.90777>
29. Li, Y., Feng, D., Wang, Z., Zhao, Y., Sun, R., Tian, D., Liu, D., Zhang, F., Ning, S., Yao, J., & Tian, X. (2019). Ischemia-induced ACSL4 activation contributes to ferroptosis-mediated tissue injury in intestinal ischemia/reperfusion. *Cell Death Differ.*, 26(11), 2284–2299. <https://doi.org/10.1038/s41418-019-0299-4>
30. Li, Z., Liu, Y., Wang, F., Gao, Z., Elhefny, M. A., Habotta, O. A., Abdel Moneim, A. E., & Kassab, R. B. (2021). Neuroprotective effects of protocatechuic acid on sodium arsenate induced toxicity in mice: Role of oxidative stress, inflammation, and apoptosis. *Chem. Biol. Interac.*, 337, 109392. <https://doi.org/10.1016/j.cbi.2021.109392>
31. Manthari, R. K., Tikka, C., Ommati, M. M., Niu, R., Sun, Z., Wang, J., Zhang, J., & Wang, J. (2018). Arsenic induces autophagy in developmental mouse cerebral cortex and hippocampus by inhibiting PI3K/Akt/mTOR signaling pathway: involvement of blood–brain barrier's tight junction proteins. *Arch. Toxicol.*, 92(11), 3255–3275. <https://doi.org/10.1007/s00204-018-2304-y>
32. Navoni, J. A., Olivera, N. M., & Villaamil Lepori, E. C. (2010). Cuantificación de arsénico por inyección en flujo-generación de hidruros-espectrometría de absorción atómica (IF-GH-EAA) previa derivatización con l-cisteína: Validación y comparación intermetodológica utilizando dos técnicas de referencia. *Acta Toxicol. Argent.*, 18(2), 29–38. [http://www.scielo.org.ar/scielo.php?script=sci\\_arttext&pid=S1851-37432010000200001&lng=es&nrm=iso&tlng=](http://www.scielo.org.ar/scielo.php?script=sci_arttext&pid=S1851-37432010000200001&lng=es&nrm=iso&tlng=)
33. Nishizaki, D., & Iwahashi, H. (2015). Baicalin inhibits the Fenton reaction by enhancing electron transfer from Fe<sup>2+</sup> to dissolved oxygen. *Am. J. Chinese Med.*, 43(01), 87–101. <https://doi.org/10.1142/S0192415X15500068>
34. Palma-Lara, I., Martínez-Castillo, M., Quintana-Pérez, J. C., Arellano-Mendoza, M. G., Tamay-Cach, F., Valenzuela-Limón, O. L., García-Montalvo, E. A., & Hernández-Zavala, A. (2020). Arsenic exposure: A public health problem leading to several cancers. *Regul. Toxicol. Pharm.*, 110, 104539. <https://doi.org/10.1016/j.yrtph.2019.104539>
35. Piloni, N. E., & Puntarulo, S. (2016). A simple kinetic model to estimate ascorbyl radical steady state concentration in rat central nervous system. Effect of subchronic Fe overload. *Bioenergetics*, 5(2), 9–11. <https://doi.org/10.4172/2167-7662.1000e125>
36. Rodríguez-Ariza, A., Toribio, F., & López-Barea, J. (1994). Rapid determination of glutathione status in fish liver using high-performance liquid chromatography and electrochemical detection. *J. Chromatog. B: Biomed. Appl.*, 656(2), 311–318. [https://doi.org/10.1016/0378-4347\(94\)00111-1](https://doi.org/10.1016/0378-4347(94)00111-1)
37. Singh, P., Verma, P. K., Sharma, P., Sood, S., & Raina, R. (2020). Oxidative changes in brain tissue after concurrent exposure to Arsenic and Quinalphos in wistar rats. *Explor. Environ. Sci. Res.*, 1(1), 87–95. <https://doi.org/10.47204/EESR.1.1.2020.087-095>

38. Stockwell, B. R., Friedmann Angeli, J. P., Bayir, H., Bush, A. I., Conrad, M., Dixon, S. J., Fulda, S., Gascón, S., Hatzios, S. K., Kagan, V. E., Noel, K., Jiang, X., Linkermann, A., Murphy, M. E., Overholtzer, M., Oyagi, A., Pagnussat, G. C., Park, J., Ran, Q., Rosenfeld, C. S., Salnikow, K., Tang, D., Torti, F. M., Torti, S. V., Toshokuni, S., Foerpel, K. A., & Zhang, D. D. (2017). Ferroptosis: A regulated cell death nexus linking metabolism, redox biology, and disease. *Cell*, 171(2), 273–285. <https://doi.org/10.1016/j.cell.2017.09.021>
39. Thakur, M., Rachamalla, M., Niyogi, S., Datusalia, A. K., & Flora, S. J. S. (2021). Molecular mechanism of Arsenic-induced neurotoxicity including neuronal dysfunctions. *Inter. J. Mol. Sci.*, 22(18), 10077. <https://doi.org/10.3390/ijms221810077>
40. Wang, H., An, P., Xie, E., Wu, Q., Fang, X., Gao, H., Zhang, Z., Li, Y., Wang, X., Zhang, J., Li, G., Yang, L., Liu, W., Min, J., & Wang, F. (2017). Characterization of ferroptosis in murine models of hemochromatosis. *Hepatology*, 66(2), 449–465. <https://doi.org/10.1002/hep.29117>
41. Wang, J. P., Qi, L., Moore, M. R., & Ng, J. C. (2002). A review of animal models for the study of arsenic carcinogenesis. *Toxicol. Lett.*, 133(1), 17–31. [https://doi.org/10.1016/S0378-4274\(02\)00086-3](https://doi.org/10.1016/S0378-4274(02)00086-3)
42. Wang, Y., Bai, C., Guan, H., Chen, R., Wang, X., Wang, B., Jin, H., & Piao, F. (2015). Subchronic exposure to arsenic induces apoptosis in the hippocampus of the mouse brains through the Bcl-2/Bax pathway. *J. Occup. Health.*, 57(3), 212–221. <https://doi.org/10.1539/joh.14-0226-OA>
43. Wei, S., Qiu, T., Yao, X., Wang, N., Jiang, L., Jia, X., Tao, Y., Wang, Z., Pei, P., Zhang, J., Zhu, Y., Yang, G., Liu, X., Liu, S., & Sun, X. (2020). Arsenic induces pancreatic dysfunction and ferroptosis via mitochondrial ROS-autophagy-lysosomal pathway. *J. Hazard. Mater.*, 384, 121390. <https://doi.org/10.1016/j.jhazmat.2019.121390>
44. World Health Statistics. (2017). WHO | World Health Statistics 2017: Monitoring health for the SDGs, suitable development goals. In World Health Organization. <https://apps.who.int/iris/handle/10665/255336>
45. Zheng, J., Zhang, K., Liu, Y., & Wang, Y. (2019). Fatal acute arsenic poisoning by external use of realgar: Case report and 30 years literature retrospective study in China. *ForensicSci. Int.*, 300, e24–e30. <https://doi.org/10.1016/j.forsciint.2019.03.012>